

Secure Image Transmission Method for UAVs Based on LoRa Technology

Pylyp Prystavka^{1,2,†}, Oksana Zolotukhina^{2,*†}, Olha Cholyshkina^{2,†}, Yevhen Filyak^{1,†}
and Mykola Zashchyk^{1,†}

¹ The State University “Kyiv Aviation Institute”, 1 Lubomyr Huzar Avenue, 03058 Kyiv, Ukraine

² Taras Shevchenko National University of Kyiv, 60 Volodymyrska Street, 01033 Kyiv, Ukraine

Abstract

This paper presents a method for secure real-time image transmission from the onboard computer of an unmanned aerial vehicle (UAV) or robotic system using LoRa (Long Range) wireless communication technology. A software architecture is proposed that ensures the acquisition, processing, encryption, and transmission of graphical data under limited hardware resources. The developed system is optimized for execution on low-power single-board computers, particularly the Raspberry Pi 4. Experimental studies confirm the effectiveness of the proposed approach for secure image transmission under constrained communication channel bandwidth. The solution is oriented toward applications in reconnaissance, monitoring, and other UAV missions, especially in environments without access to GPS or the Internet.

Keywords

LoRa, UAV, image transmission, secure communication, real-time data, edge computing, embedded systems, encryption.

1. Introduction

Unmanned aerial vehicles (UAVs) are playing an increasingly important role across various domains—from environmental monitoring and agriculture to military and rescue operations. In real-time scenarios, the transmission of visual information from a UAV to a ground control station is often critical for making operational decisions. However, in most deployment cases, particularly in isolated or radio-constrained environments, traditional high-bandwidth communication channels such as LTE, Wi-Fi, or Starlink are unavailable, unstable, or excessively power-consuming.

In such cases, an energy-efficient solution is the use of LoRa (Long Range) wireless technology, which enables long-distance data transmission with low power consumption. Nevertheless, LoRa's extremely limited bandwidth poses significant challenges for image transmission, especially in real time. Furthermore, when UAVs are employed in security-sensitive applications such as defense or critical infrastructure protection, the confidentiality and integrity of transmitted visual data become crucial.

In response to these challenges, this work focuses on developing a method for secure image transmission from UAVs using LoRa, aiming to balance channel limitations, energy efficiency, and information security requirements. The proposed approach incorporates efficient image

Information Technology and Implementation (IT&I-2025), November 20-21, 2025, Kyiv, Ukraine

*Corresponding author.

†These authors contributed equally.

✉ chindakor37@gmail.com (P.Prystavka); oksana.zolotukhina@knu.ua (O.Zolotukhina), olha.cholyshkina@knu.ua (O.Cholyshkina); yevhen.filyak@kai.edu.ua (Y.Filyak); 6293404@stud.kai.edu.ua (M. Zashchyk)

🆔 0000-0002-0360-2459 (P.Prystavka); 0000-0002-3314-417X (O.Zolotukhina), 0000-0002-0681-0413 (O.Cholyshkina); 0009-0006-6141-943X (Y.Filyak)



© 2025 Copyright for this paper by its authors. Use permitted under Creative Commons License Attribution 4.0 International (CC BY 4.0).

preprocessing algorithms, fragmentation, compression, and symmetric encryption, all of which can be executed on resource-constrained onboard computers.

The objective of this study is to design a method for secure real-time image transmission from a UAV's onboard computer using LoRa wireless technology, while accounting for limited hardware resources and energy-efficiency requirements.

The proposed technology ensures image transmission even under ultra-low channel rates (down to several kilobits per second), making it applicable in remote or hostile environments without sacrificing basic functionality. The research findings can be applied in the development of adaptive distributed surveillance systems, as well as in autonomous navigation and real-time response projects.

Due to its energy efficiency and long transmission range, LoRa technology is widely adopted in Internet of Things (IoT) systems for data transfer in resource-constrained environments. However, transmitting images under such conditions remains a challenging task because of narrow bandwidth, which restricts the amount of data transferred and complicates integrity assurance.

In [1], image transmission in agricultural monitoring systems using LoRa is discussed, emphasizing the need for preprocessing such as resolution reduction, grayscale conversion, and JPEG compression. The authors also highlight the importance of adapting the transmission rate to network conditions.

Another approach is presented in [2], where a multi-layer communication framework is proposed for efficient image transmission. This method allows image transfer via LPWAN by adapting compression to the available bandwidth. The authors stress that even with simple compression methods (e.g., JPEG), performance heavily depends on segmentation strategy.

In [3], experiments confirmed the feasibility of transmitting training samples (images) over LoRa for edge learning systems using simple compression and prior scaling. Despite delays, the experiments demonstrated effective preservation of model classification quality.

The study [4] analyzed the reliability of image transmission over LoRa in urban environments. The authors implemented a simple Automatic Repeat reQuest (ARQ) mechanism to compensate for data losses, improving image reconstruction completeness at low error rates.

From a network architecture perspective, [5] proposed a hybrid architecture based on drones deploying LoRaWAN nodes in real time. This approach enables network deployment in hard-to-reach areas, including image transmission, but does not address optimization of onboard UAV data processing.

The survey [6] provides a detailed analysis of LoRa in Flying Ad Hoc Networks (FANETs). The authors discussed challenges such as high transmission latency and small packet size, which critically affect UAV image transmission.

In [7], attention is drawn to image compression methods in LoRa-enabled sensor nodes. The authors highlight the relevance of adaptive methods depending on context (lighting, scene dynamics, etc.), which significantly influence data quality. However, these methods do not consider the constraints of UAV onboard computational resources.

Finally, [8] demonstrated the advantages of combining compression with cryptographic approaches optimized for LPWAN. This combination reduces data volume while enhancing security, but does not explore symmetric encryption under limited onboard processing power.

The analysis of the reviewed works highlights the growing interest in using LoRa technology for visual data transmission under limited bandwidth and energy constraints. A significant portion of existing solutions focuses on agriculture, environmental monitoring, or industrial IoT scenarios. However, the specific requirements of autonomous UAVs [10]—such as real-time operation, data security, and execution on constrained computing platforms—remain insufficiently addressed. Current studies lack comprehensive solutions that integrate adaptive image compression, symmetric encryption, and optimization for ARM-based architectures. This gap motivates further research and justifies the relevance of the proposed approach.

2. Materials and Methods

LoRa is a proprietary physical-layer technology that employs chirp spread spectrum (CSS) modulation to ensure reliable communication under low signal-to-noise ratio (SNR) conditions. Due to pseudorandom encoding, the signal gains a significant processing gain, which enables its recovery even in the presence of interference. These properties make LoRa suitable for deployment on unmanned aerial vehicles, where energy efficiency, resistance to interference, and long-distance transmission capabilities are of critical importance. In this study, LoRa is applied to secure real-time image transmission under computational and energy constraints.

LoRa supports three different bandwidth options: 125 kHz, 250 kHz, and 500 kHz. One of its key parameters is the Spreading Factor (SF), which defines the number of distinct symbols that can be transmitted. For instance, when SF = 7, the total number of possible symbols equals 128 (2^7). The following formula [12] describes the generation of a LoRa signal:

$$c(nT_s + kT) = \frac{1}{\sqrt{2^{\text{SF}}}} e^{(j2\pi(s(nT_s) + k) \bmod 2^{\text{SF}}) \frac{k}{2^{\text{SF}}}}, \quad (1)$$

where nT_s is the discrete time index, T_s is the duration of a single sample. The variable n is used for time increments. The function $s(nT_s)$ defines the chirp frequency as a function of time and encodes the transmitted information through frequency shifts. The term kT represents an additional time offset. The operation $\bmod 2^{\text{SF}}$ is forming the basis of chirp signal generation. The factor $\frac{1}{\sqrt{2^{\text{SF}}}}$ is a normalization coefficient that maintains signal energy stability. Since the function is exponential in nature, it represents a complex base function. In this context, the variable k is incremented for each symbol/chirp. Each symbol S value generates a distinct waveform.

The next task of the receiver is to interpret the symbols and perform de-chirping. From a mathematical perspective, correlation is a key mechanism for de-chirping the received signal. Essentially, the method evaluates the similarity of each symbol and determines the coefficient with the highest correlation. This process may be computationally intensive, as the receiver must first successfully capture the symbol and then verify its similarity. However, mathematical optimizations significantly simplify this procedure. Another advantage of using correlation is that it enables demodulation of signals even when they are below the noise floor.

$$C(m) = \sum_{n=0}^{2^{\text{SF}}-1} r(nT_s) c_m^*(nT_s), \quad (2)$$

where $r(nT_s)$ is received signal, $c_m^*(nT_s)$ is complex-conjugate reference symbols, $C(m)$ is correlation coefficient for the hypothesis "symbol=m". Then m is chosen for which $|C(m)|$ is maximal.

The summation over k , ranging from 0 to $2^{\text{SF}}-1$, allows for calculating the correlation coefficient for each symbol within the value space defined by the spreading factor (SF). This makes it possible to identify the symbol most similar to the received signal, even under low signal-to-noise ratio conditions. Such an approach ensures LoRa's robustness against interference and its effectiveness in decoding.

The physical layer of LoRa consists of the following components [12]: 8 preamble symbols, 2 synchronization symbols, the payload, and an optional cyclic redundancy check (CRC). This structure enables efficient data transmission and proper synchronization between transmitter and receiver. The preamble symbols form the initial part of the signal, consisting of 8 consecutive up-chirps. Their primary function is to ensure LoRa signal detection by the receiver and initiate data processing. They are followed by 2 down-chirps (chirps with decreasing frequency), which serve as synchronization symbols. Their role is to align the receiver precisely in time and frequency for accurate payload decoding. The payload is transmitted as modulated symbols encoded by chirps. The frequency shifts of these chirps represent the encoded symbols that carry the transmitted data. When CRC is included, the receiver can verify the integrity of the received data and detect errors caused by interference.

The relationship between the symbol rate (R_s), bandwidth (BW), and spreading factor (SF) is expressed by the equation [12]:

$$R_s = \frac{BW}{2^{SF}}. \quad (3)$$

A higher spreading factor (SF) results in a longer time-on-air, which increases transmission range and resistance to noise but reduces the data rate. In contrast, a lower SF provides a higher data rate at the expense of reduced robustness and shorter transmission distance.

The proposed UAV image transmission system consists of two main components: the transmitting unit (onboard UAV) and the receiving unit (ground station). The transmitting unit, installed on the UAV, includes an image acquisition module (camera), a Raspberry Pi 4 single-board computer, a LoRa wireless transceiver (SX1278), and a microSD storage device for local data saving. The receiving unit, located at the ground station, can be implemented on a personal computer or another compatible device equipped with an SX1278 module. It provides data reception, verification, decryption, and storage of the received information.

Image transmission is implemented using scripts that handle preprocessing, encryption, modulation, and signal transfer via a Wi-Fi connection established through a mobile device. The transmitter is represented by the Raspberry Pi 4, while the receiver is a computer.

The transmission process consists of several stages. First, the image is divided into an appropriate number of channels, after which the transmitted information is encrypted using AES-CTR [13] to ensure security. Next, chirps are generated for each image pixel or text symbol. Noise is then modeled in the channel to create more realistic transmission conditions. This not only allows optimization of the transmission process but also enables verification of algorithm robustness under near-real-world conditions. Finally, the program decodes the received chirps and reconstructs the original image or text.

The reception process is organized to ensure accurate recovery of transmitted data. Through the generation of inverse chirps and analysis of the frequency spectrum of the received signals, chirps are demodulated into symbols, which are subsequently decrypted to restore the original texts or images. To handle different data types—color images, grayscale images, or text—specialized modules are employed, providing adaptability of the system.

The experimental study consisted of three stages (Fig. 1). Five image resolutions were selected for testing: 64×64 , 128×128 , 256×256 , 512×512 , and 1920×1080 pixels [11]. The statistical sample size was set to 1000 transmission–reception iterations, except for the largest resolution (1920×1080), where a reduced number of iterations was applied due to data volume.

The experiment begins with the configuration of an access point, which serves as the initial step for establishing a connection between the transmitting device (computer) and the Raspberry Pi 4. Both devices were connected to the same local network.

The second stage involves data preparation on the transmitter side. At this stage, transmission parameters are initialized, including the selection of system settings, such as the scaling factor. Next, the image to be transmitted and a text message are selected.

In the following stage, a transmission script is launched, which generates chirps encoding the selected image and message. Simultaneously, a reception script is activated on the receiving device to ensure data acquisition, decoding, and storage of the received image along with statistical information.

After the data transmission process is completed, the obtained results are analyzed. This stage includes executing scripts for constructing histograms of relative transmission and reception times, as well as calculating key performance metrics such as Peak Signal-to-Noise Ratio (PSNR) and Structural Similarity Index (SSIM), along with computing the median, mean, and standard deviation.

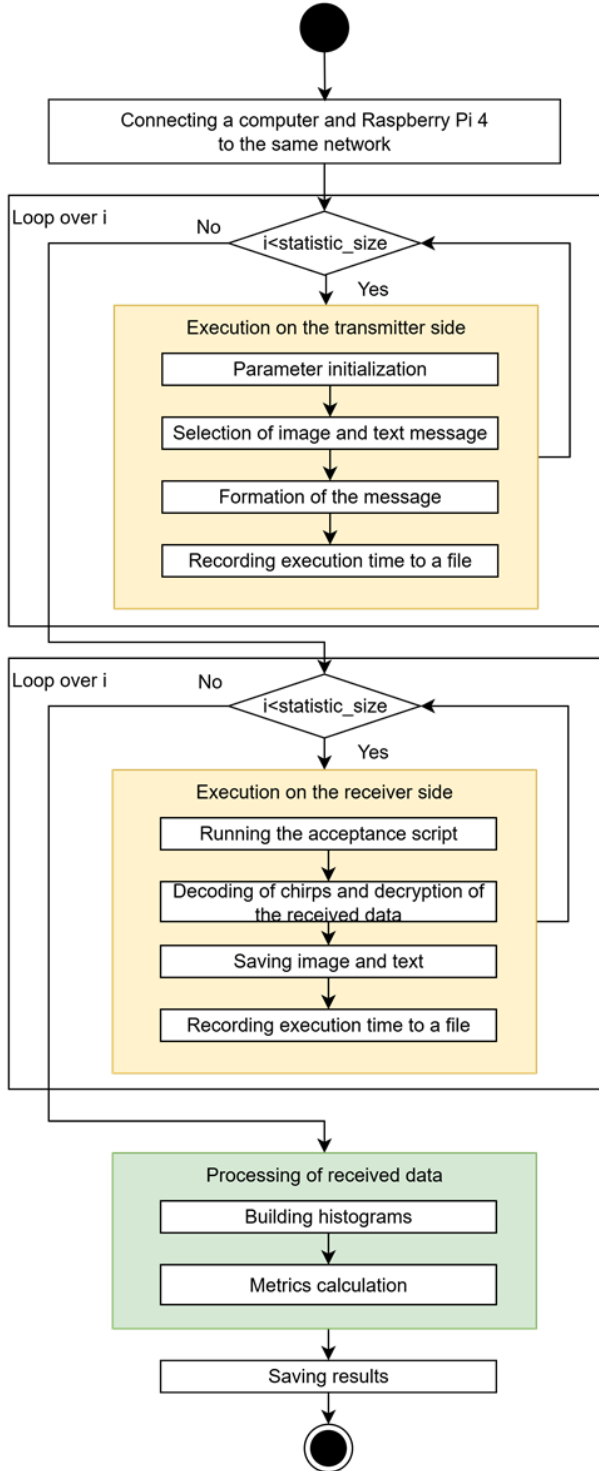


Figure 1: Scheme of the experiment

3. Result and Discussion

Two transmission modes were tested: a high-accuracy mode, which provides maximum image quality, and a high-speed mode, where images are pre-scaled. In the high-accuracy mode, the image scaling factor is set to 1, meaning that the image size remains unchanged. Statistical data for this mode were collected for four image resolutions: 64×64 , 128×128 , 256×256 , and 512×512 , with 1000 transmission-reception iterations for each. For the 1920×1080 resolution, 50 iterations were conducted due to the large data size.

An example histogram of the relative frequency distribution of transmission/reception times for the 128×128 resolution is shown in the Fig. 2, 3.

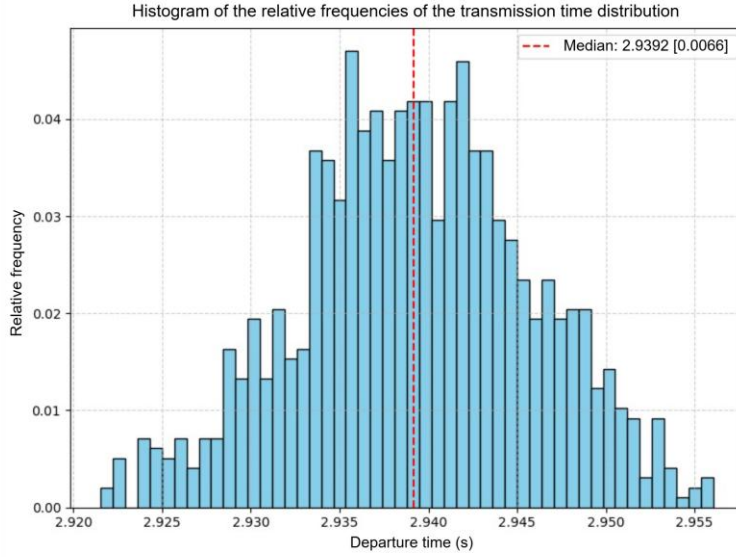


Figure 2: Relative frequencies of transmission time for a 128×128 color image.

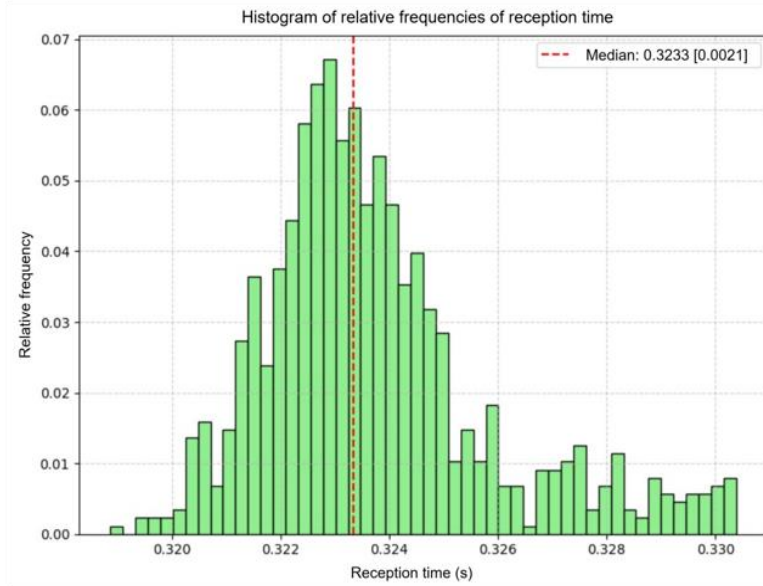


Figure 3: Relative frequencies of reception time for a 128×128 color image.

For all images in the experiment, the PSNR value was equal to 361, and the SSIM value was 1. The deviations in both cases were 0. This indicates that all images were transmitted without distortion, regardless of their size, which corresponds to the conditions of lossless transmission.

According to the experimental results (Tables 1–3), a significant difference in transmission duration was observed for images with a resolution of 512×512 . On average, transmission required 3.25 seconds, while reception took 5.14 seconds with a deviation of 0.12. This jump can be considered a threshold, which represents the main distinction between high-accuracy and high-speed transmission modes.

For testing the high-speed transmission mode, images with a resolution of 1920×1080 pixels were used. The high-speed mode implies the transmission of downsampled images [9]. In this way, even large-resolution images can be transmitted relatively quickly. The main drawback of this mode,

however, is the reduction in image quality. Thus, the primary task is to identify scaling values that enable faster transmission while minimizing the loss of details.

Based on the data obtained from high-accuracy transmission experiments, a noticeable jump occurs after reaching the 512×512 resolution. Therefore, the most suitable options are scaling by a factor of 4—since a 480×270 image contains approximately half as many pixels as 512×512 —and scaling by a factor of 10.

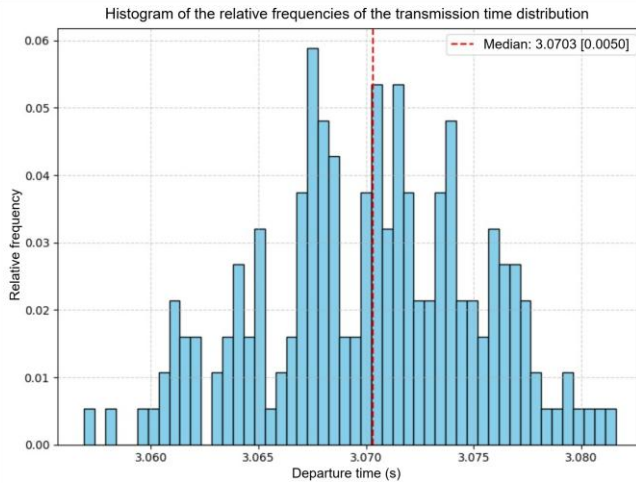


Figure 4: Relative frequencies of transmission time for a 1920×1080 color image (a 4-fold decrease).

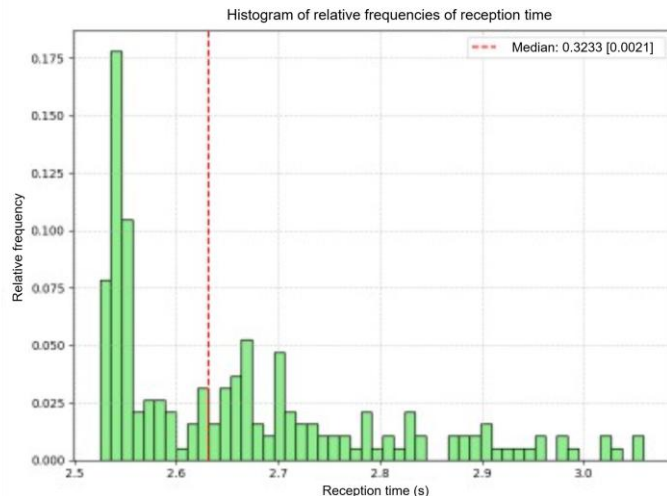


Figure 5: Relative frequencies of reception time for a 920×1080 color image (a 4-fold decrease).

The values of 3.07 seconds for transmission and 2.63 seconds for decoding of color images also fall within the expected range. The corresponding metrics are as follows: PSNR = 25.71 dB, SSIM = 0.72. This indicates a relatively fast transmission method that still provides good image quality.

Experimental results further demonstrated that downscaling images by a factor of 10 does not yield a time advantage; instead, it significantly reduces image quality. The average transmission time in this case was 2.94 seconds, with a reception time of 0.43 seconds. The corresponding metrics were: PSNR = 22.67 dB, SSIM = 0.57. In fact, transmitting a 256×256 color image without downscaling proves to be more efficient.

The summary of all experimental results for the tested image sizes is presented in the tables below. As noted earlier, transmission was performed using a Raspberry Pi 4 as the sender, with a computer serving as the receiver.

Table 1

Median times for images of different sizes

Image size	Transmission time (color), s	Reception time (color), s	PSNR	SSIM
64×64	2.89	0.09	361.2	1.0
128×128	2.94	0.32	361.2	1.0
256×256	2.98	1.33	361.2	1.0
512×512	3.26	5.16	361.2	1.0
1920×1080 (without reduction)	5.65	41.05	361.2	1.0
1920×1080 (4x reduction)	3.07	2.64	25.71	0.72
1920×1080 (10x reduction)	2.94	0.43	22.67	0.57

Table 2

Average time values for images of different sizes

Image size	Transmission time (color), s	Reception time (color), s	PSNR	SSIM
64×64	2.90	0.09	361.2	1.0
128×128	2.94	0.33	361.2	1.0
256×256	2.98	1.36	361.2	1.0
512×512	3.26	5.26	361.2	1.0
1920×1080 (without reduction)	5.65	41.14	361.2	1.0
1920×1080 (4x reduction)	3.07	2.67	25.71	0.72
1920×1080 (10x reduction)	2.95	0.44	22.67	0.57

Table 3

Root mean square deviations of time for images of different sizes

Image size	Transmission time (color), s	Reception time (color), s	PSNR	SSIM
64×64	0.02	0.01	361.2	1.0
128×128	0.01	0.014	361.2	1.0
256×256	0.007	0.098	361.2	1.0
512×512	0.008	0.23	361.2	1.0
1920×1080 (without reduction)	0.046	0.43	361.2	1.0
1920×1080 (4x reduction)	0.022	0.18	25.713	0.717
1920×1080 (10x reduction)	0.027	0.04	22.665	0.569

4. Conclusions

Based on the analysis of the results, the following conclusions can be drawn. Computational processes on both the transmitter and receiver sides significantly influence transmission time, leading to observable fluctuations and deviations from the median and mean values. For example, the overhead associated with encryption, chirp encoding, and data preparation may be uneven due to the specifics of processor operation.

It can also be concluded that the optimal downscaling factor is 4. This provides a balance between image quality and transmission speed. For large images such as 1920×1080 , scaling down by a factor of 4 reduces the reception time of grayscale images to 0.89 seconds (compared to 13.40 seconds without downscaling) and color images to 2.64 seconds (instead of 41.05 seconds). At the same time, the quality remains acceptable: $\text{PSNR} \approx 25.71$, $\text{SSIM} \approx 0.72$. Scaling by a factor of 10, while further reducing transmission time, results in a significant deterioration in quality: PSNR drops to 22.67, and SSIM to 0.57. Such values are insufficient for tasks requiring high levels of detail.

Another noteworthy observation is that transmission time increases very slowly. Specifically, the time required to transmit 64×64 images is nearly the same as for 512×512 images. This behavior is related to the mechanism of chirp preparation. For all images, chirps are precomputed for every unique pixel intensity value. Once a chirp is generated for a given value, it is stored in a dictionary and reused, rather than recalculated. Consequently, the increase in transmission time depends not so much on image resolution, but on the number of unique intensity values present.

In the context of implementing LoRa technology for transmitting video frame fragments from the onboard or target camera of an unmanned aerial vehicle (UAV), it is necessary to consider the influence of various environmental factors, including extreme weather conditions, electromagnetic interference, and the specific characteristics of urban and rural environments, which are critically important for UAV operation in isolated areas. Within the scope of this study, the LoRa transmission channel is considered as a logical extension of the existing UAV control channel operating on standard frequencies, rather than as an independent task of integrating LoRa technology into the drone. The main focus is placed on evaluating the temporal characteristics of transmission and reception processes, as well as the quality of the transmitted images, while the specific hardware implementation depends on the configuration of the particular UAV platform and the characteristics of its communication equipment. Such experiments are planned for subsequent research stages during the advancement of the technology to Technology Readiness Level (TRL) 6 and higher.

It is well known that the communication range of LoRa significantly depends on environmental conditions. In urban environments with numerous obstacles, such as buildings, stable communication can typically be maintained over distances of 2–5 km, and, with optimal antenna placement and frequency selection, up to 10 km. In rural areas with fewer obstacles, the effective range may reach 5–15 km, while under ideal conditions it can extend to 20 km or more. In open areas, such as over water or in desert regions, the achievable range can exceed 30 km. At the same time, the quality and stability of signal transmission are affected by parameters such as transmitter power, receiver sensitivity, operating frequency, and antenna type.

In the experimental part of this research, a Wi-Fi-based channel was used to ensure the stability and reproducibility of results. This approach made it possible to achieve Technology Readiness Level (TRL) 5, confirming the feasibility of the proposed method under controlled laboratory conditions. Further tests using LoRa technology are planned to be conducted at specialized testing grounds once restrictions on flight experiments—imposed by the ongoing martial law in Ukraine—are lifted.

Finally, it should be noted that despite LoRa's high resistance to noise and interference, the technology remains vulnerable to targeted actions by electronic warfare (EW) systems, particularly jamming. Therefore, future research directions include the development of combined methods aimed at enhancing interference immunity and resilience against active electronic countermeasures.

Declaration on Generative AI

During the preparation of this work, the authors used CahtGPT-4o in order to: Grammar and spelling check. After using this tool, the authors reviewed and edited the content as necessary and bears full responsibility for the content of the publication.

References

- [1] Chen Tonghao, Eager Derek, Makaroff Dwight. "Efficient Image Transmission Using LoRa Technology in Agricultural Monitoring IoT Systems." 2019 IEEE International Conference on Internet of Things (iThings), Green Computing and Communications (GreenCom), CPSCom/SmartData, 2019. DOI: 10.1109/iThings/GreenCom/CPSCom/SmartData.2019.00166.
- [2] Chaparro Fabián B., Pérez Manuel, Mendez Diego. "A Communication Framework for Image Transmission through LPWAN Technology." *Electronics*, vol. 11, no. 11, 2022, Article 1764. DOI: 10.3390/electronics11111764.
- [3] Edirisinghe Sampath, Sachinda Imesh. "Image Transmission Using LoRa for Edge Learning." *SSRN*, 16 Feb. 2024. DOI: 10.2139/ssrn.4728960.
- [4] Reliable image transmission over LoRa networks (J. Kim et al.). *Issues in Information Systems*, Vol. 25, Issue 1, 2024, pp. 199-207.
- [5] H. Zhao et al. "Design and Implementation of a Novel UAV-Assisted LoRaWAN Network." *Drones*, vol. 8, no. 10, 2024, Article 520.
- [6] W. D. Paredes, H. Kaushal, I. Vakilinia, Z. Prodanoff. "LoRa Technology in Flying Ad Hoc Networks: A Survey of Challenges and Open Issues." *Sensors (Basel)*, vol. 23, no. 5, Article 2403, 2023. DOI:10.3390/s23052403.
- [7] D. I. Săcăleanu, R. Popescu, I. P. Manciu, and L. A. Perișoră. Data Compression in Wireless Sensor Nodes with LoRa. Proceedings of the "Electronics, Computers and Artificial Intelligence (ECAI) Conference", Iași, Romania, November 2019. Available at: https://www.researchgate.net/publication/332446815_Data_Compression_in_Wireless_Sensor_Nodes_with_LoRa
- [8] Anthony Feijoo-Añazco, Dan García-Carrillo, Jesús Sánchez-Gómez, Rafael Marín-Pérez. Innovative Security and Compression for Constrained IoT Networks. *Internet of Things*, vol. 24, 100899, 2023. DOI: 10.1016/j.iot.2023.100899.
- [9] P. Prystavka, O. Cholyshkina, Pyramid Image and Resize Based on Spline Model стаття (scopus) *International Journal of Image, Graphics and Signal Processing(IJIGSP)*, Vol.14, No.1, pp. 1-14, 2022. DOI: 10.5815/ijigsp.2
- [10] P. Prystavka, A. Chyrkov, Suspicious Object Search in Airborne Camera Video Stream // In: Z., Hu, S., Petoukhov, I., Dychka, M., He (eds) *Advances in Computer Science for Engineering and Education. ICCSEEA 2018. Advances in Intelligent Systems and Computing*, vol. 754. Springer, Cham, 2018. – P. 340–348. – DOI: 10.1007/978-3-319-91008-6_34
- [11] V. Zivakin, O. Kozachuk, P. Prystavka, O. Cholyshkina, Training set AERIAL SURVEY for Data Recognition Systems From Aerial Surveillance Cameras // *CEUR Workshop Proceedings*. – 2022. – Vol. 3347. – P. 246–255. – [Online]. Available: https://ceur-ws.org/Vol-3347/Paper_21.pdf.
- [12] K. Peppas, A. Alexiou, G. Kalivas, New Results for the Error Rate Performance of LoRa, *Sensors* 22(9) (2022) 1–20. <https://doi.org/10.3390/s22093258>.
- [13] W.K. Lee, Speed Record of AES-CTR and AES-ECB Bit-Sliced Implementations, *IEEE Embedded Systems Letters* (2024). <https://doi.org/10.1109/LES.2024.3409725>.